Article

Journal of
Nanoscience and Nanotechnology
Vol. 18, 4371–4379, 2018
www.aspbs.com/jnn

Fabrication of Electrochemical Biosensor with ZnO-PVA Nanocomposite Interface for the Detection of Hydrogen Peroxide

Navin Kishore Sekar[1,2], Manju Bhargavi Gumpu[1,3], Bhat Lakshmishri Ramachandra[1,3], Noel Nesakumar[1,3], Prabakaran Sankar[1,3], K. Jayanth Babu[1,3], Uma Maheswari Krishnan[1,2], and John Bosco Balaguru Rayappan[1,3,*]

[1]*Centre for Nanotechnology and Advanced Biomaterials, SASTRA University, Thanjavur 613401, Tamil Nadu, India*
[2]*School of Chemical and Biotechnology,* [3]*School of Electrical and Electronics Engineering, SASTRA University, Thanjavur 613401, Tamil Nadu, India*

Hydrogen peroxide (H_2O_2) is considered to be highly toxic and its increased concentration in human body may lead to diseases like alzheimer's, parkinson's, cardiovascular, tumor and cancer. Hence, there is an increasing demand for the detection of H_2O_2 in human blood serum. In this context, an electrochemical sensor was developed using zinc oxide-polyvinyl alcohol (ZnO-PVA) nanocomposite as a nano-interface. The fabricated Au/ZnO-PVA/CAT/Chitosan bio-electrode exhibited a well-defined redox peak with anodic and cathodic peak potential of −0.408 V and 0.259 V for Fe(III):Fe(II) and H_2O_2:1/2 O_2 redox couples respectively. The developed biosensor exhibited a linear range of 1 μM–17 μM with a sensitivity of 210.49 μA μM^{-1} cm^{-2}, response time of less than 1 s, limit of detection of 9.13 nM and a limit of quantification of 30.13 nM. The developed bio-electrode showed a Michaelis-Menten constant (K_M) of 0.39 μM and dry stability of 93% up to 20 days. The obtained biosensor was successfully utilized to determine the H_2O_2 concentration in human blood serum sample.

Keywords: Catalase, Nano-Interface, ZnO-PVA, Electrochemical Biosensor, H_2O_2, Blood Serum Analysis.

1. INTRODUCTION

In human system, hydrogen peroxide (H_2O_2) plays an important role in regulating cellular processes such as vascular remodeling, activation of immune cells and apoptosis.[1] H_2O_2 is the end product of many biochemical reactions catalyzed by large number of oxidase enzymes and plays a major role in environmental, pharmaceutical and food analysis.[1] Increase in the level of H_2O_2 production in humans induces cytotoxic effects, which results in cell damage associated with the initiation and propagation of many diseases.[1] The increased concentration of H_2O_2 in human body may lead to diseases like alzheimer's, parkinson's, cardiovascular, tumor and cancer. Owing to these ill effects, H_2O_2 detection using biosensor has an immense value in clinical applications.

Till date, H_2O_2 quantification is being carried out using analytical methods such as raman spectroscopy,[2,3] infrared spectrometer,[4] mass spectrometry,[5] chemiluminescence,[6] colorimetric detection[7] and fluorescence imaging.[8] Generally, these techniques are complex, time-consuming and expensive. In order to overcome these drawbacks, electrochemical sensors[9–12] are preferred because of their lower cost of analysis and response time, better sensitivity and simple to operate. H_2O_2 detection is done via enzymatic and non-enzymatic modes.[13–22] In order to provide effective low cost analysis with prolonged stability, non-enzymatic approach for the electrochemical detection of H_2O_2 has gained attraction in recent years. Generally, the materials used for sensing electrocatalytic H_2O_2 are silver wires, ferrocene carboxylic acid, nonporous carbon, Fe@Pt core–shell nanoparticles, bis (acetylacetonate) oxovanadium(IV) complex, CuO@Cu_2O nanowires and nanoporous copper.[13–19] But the major drawbacks of using

*Author to whom correspondence should be addressed.

these materials as sensing elements are lack of specificity and stability in alkaline and neutral solutions. To overcome these issues, enzymatic sensors are preferred in enhancing the specificity and stability. The commonly used enzymes in H_2O_2 biosensors are heme proteins such as catalase (CAT),[9,11] cytochrome c (Cyt c),[20] hemoglobin (Hb),[21] myoglobin (Mb).[21] The iron group present in these heme proteins undergo oxidation and reduction over a different range of potentials catalyzing the H_2O_2 into water and oxygen.[22] Wang et al.[23] investigated the catalytic activity of CAT, Hb and Mb in oxidation of H_2O_2 to O_2 and H_2O. In this, CAT enzyme showed higher affinity, higher turnover number, greater specificity and better sensitivity than Hb and Mb. Hence in this work, catalase enzyme was preferred as electrocatalyst for the oxidation of H_2O_2.

In nanomaterial free matrices of H_2O_2 biosensor, sensitivity, limit of detection (LOD) and electron transfer rate (K_s) between CAT and working electrode are poor. To improve the electron transfer between CAT and working electrode, nano-interface was introduced. Nano-interfaces namely gold nanoparticles, ceria, iron oxide nanoparticles, multi-walled carbon nanotubes, zinc oxide (ZnO) were used towards the detection of H_2O_2.[24–27] Among various nano-interfaces, nanostructured ZnO are widely employed in the fabrication of electrochemical biosensors. The performance of ZnO based electrochemical H_2O_2 biosensors primarily depends on the size and shape of ZnO nano-interface.[28–31] Until now, complex multiple fork, sphere, rod and flower-like morphologies of ZnO nanostructures have been employed in the fabrication of electrochemical H_2O_2 biosensors.[28–31] Yang et al.[28] fabricated H_2O_2 biosensor by immobilizing horseradish peroxidase (HRP) enzyme on complex multiple fork-like ZnO nano-interface modified glassy carbon electrode in which ZnO nano-interface provided high electroactive surface area and rigid framework for HRP enzyme and thereby enhanced electron transfer rate was achieved. Besides, Zhang et al.[29] developed H_2O_2 biosensor based on synergist effect of using flower-like ZnO crystals and gold nanoparticles in which flower-like ZnO crystals facilitated sensitive, direct and rapid determination of H_2O_2 at low working potential owing to its high electron transfer rate and HRP immobilization efficiency. As a step of advancement, Tan et al.[30] and Li et al.[31] developed H_2O_2 biosensor based on ZnO nanorods/poly vinyl alcohol (ZnO/PVA) composite and Sb-doped ZnO microsphere films respectively in which ZnO nanorods and microspheres provided biocompatible nano-environment for hemoglobin (Hb) and HRP to orient the active sites towards H_2O_2 due to their high isoelectric point difference between nano-ZnO and immobilized enzyme. Since ZnO nanoparticles have high electronic conductivity, large surface area, high catalytic activity, electron transfer property and high isoelectric point, ZnO nanoparticles were preferred in this work.

Further to enhance the conductivity of ZnO nanoparticle, PVA was electrospun with ZnO to form ZnO-PVA nanocomposites. Here, PVA provides electrical conductivity to ZnO-polymer hybrid nanocomposite film and facilitates high electron density to the bioelectrode surface by free –OH groups, which offer high resistance towards anionic interferents in the human blood serum samples.[32] Moreover, ZnO-PVA nanocomposite exhibited good mechanical stability with flexible surfaces, which helps to immobilize a large amount of CAT enzyme. This in-turn helped to obtain rapid electrochemical response towards H_2O_2. In addition, PVA acts as a localization layer for electronic transition between CAT and ZnO, which helped in lowering the response time.[32] To the best of our knowledge, this is the first time zinc oxide-polyvinyl alcohol nanocomposite (ZnO-PVA) is being utilized for the electrochemical detection of H_2O_2 detection in human blood serum samples.

2. MATERIALS AND METHODS

2.1. Reagents and Materials

CAT enzyme from bovine liver, lyophilized powder (2000–5000 U mg^{-1}), sodium hydroxide, 0.5 wt% of chitosan in 1% of acetic acid (molecular weight: 140,000 g mol^{-1}), ascorbic acid, glucose, lactic acid, monobasic sodium phosphate monohydrate and dibasic sodium phosphate dihydrate were purchased from Merck India Ltd., India. Other chemicals namely hydrogen peroxide, urea, zinc acetate dihydrate ($Zn(CH_3COO)_2 \cdot 2H_2O$) (molecular weight: 219.61 g mol^{-1}) and polyvinyl alcohol (molecular weight: 14,000 g mol^{-1}) were purchased from Sigma aldrich., India. 0.1 M KCl saturated Ag/AgCl reference electrode (CHI111, 0.5 mm diameter), Au electrode (CHI101, 2 mm diameter) and platinum wire counter electrode (CHI115, 0.5 mm diameter) were purchased from CH Instruments, Inc., USA. All reagents and solutions were prepared using deionized water (AQUA purifications systems, India).

2.2. Synthesis of ZnO Nanocomposites

PVA (1 g) was added into a 10 mL deionised water and the solution was stirred for 30 min. Subsequently, zinc acetate (1 g) was added to the solution. Then the solution was heated and stirred at 393 K for 1 h and it was allowed to cool at room temperature. For the preparation of electrospun ZnO-PVA nanocomposites, the stirred composite solution was transferred to the 5 mL glass syringe and the syringe was fitted to the electrospinning setup with a blunt needle of 24 G. The experimental conditions such as tip to target distance, flow rate and applied voltage were maintained at 12 cm, 0.001 mL min^{-1} and 15 kV respectively for the electrospinning process. Consequently, the obtained nanofibers were collected on the static collector.

2.3. Characterization Techniques

Structural and morphological properties of the prepared ZnO-PVA nanofibers were characterized using X-ray

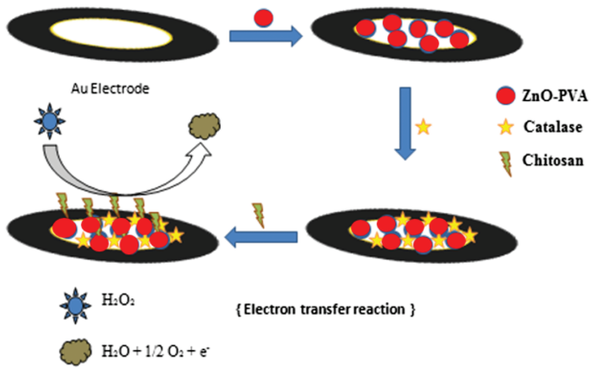

Figure 1. Fabrication of Au/ZnO-PVA/CAT/Chitosan bio-electrode.

diffractometer (D8 Focus, Bruker, Germany) with Cu Kα ($\lambda = 0.1546$ nm) and field emission scanning electron microscope (FE-SEM, Model JSM 6701F, JEOL, Japan) respectively. Fourier Transform Infrared Spectrometer (FT-IR, Model spectrum 100, Perkin Elmer, USA) was used to confirm the immobilization of CAT on ZnO-PVA nanocomposites.

2.4. Fabrication of Au/ZnO-PVA/CAT/Chitosan Bio-Electrode

Prior to the fabrication, Au working electrode was polished with alumina powder (0.05 μm). 0.05 mg of ZnO-PVA nanocomposite was taken in an eppendorf and suspended in 100 μL of PBS. Then, the nanocomposite was sonicated for 1 h to get a finely dispersed solution. Further, CAT (1000 U mL^{-1}) and chitosan (100 μL) were added to the PBS solution and sonicated for 2 min. Later, 3 μL of the dispersed solution was taken and immobilized onto the Au working electrode surface and allowed to dry at room temperature for 3–4 h (Fig. 1). The modified working electrode was then used for further experiments.

2.5. Electrochemical Analysis

Electrochemical workstation (CH1600C, CH Instruments, USA) was used to analyze the electrochemical measurements. The three electrode system comprised of Au/ZnO-PVA/CAT/Chitosan as working electrode, Ag/AgCl saturated with 0.1 M KCl as a reference electrode and platinum wire as an auxiliary electrode. All cyclic voltammetry experiments were carried out with 5 mL PBS solution in a 20 mL electrochemical cell. All cyclic voltammetry studies were performed in a potential range from 0.4 V to −1.0 V at room temperature.

3. RESULTS AND DISCUSSION

3.1. Structural and Morphological Studies of ZnO-PVA Nanocomposites

The morphologies of ZnO-PVA, ZnO-PVA/CAT and ZnO-PVA/CAT/Chitosan were characterized using FE-SEM (Figs. 2(a–c)). As shown in Figure 2(a), the ZnO-PVA nanocomposites exhibited a flake-like morphology composed of small irregular nanoparticles with very rough surface. The flake-like morphology owned high surface area and could provide an excellent adsorption for CAT enzyme. On adding CAT to the ZnO-PVA nanocomposite, the FE-SEM image of ZnO-PVA/CAT displayed brick-like morphology with irregular shape (Fig. 2(b)). On adding chitosan membrane further to the surface of ZnO-PVA/CAT nanocomposite, the surface of ZnO-PVA/CAT was covered with thin layer of chitosan membrane which resulted in smooth and featureless morphology (Fig. 2(c)). Moreover, particle size distributions of ZnO-PVA and ZnO-PVA/CAT were calculated from the selected FE-SEM images using ImageJ 1.49p software. The diameter of ZnO-PVA nanocomposites ranged from 0.24 μm to 1.29 μm with mean diameter of 0.69 ± 0.54 μm. The length and height of ZnO-PVA/CAT were estimated as 1.93 ± 1.11 μm and 1.16 ± 0.55 μm respectively.

3.2. FT-IR Study

FT-IR spectrum of ZnO-PVA/CAT/Chitosan is shown in Figure 2(d). Due to inter-atomic vibrations, the absorption peak of metal oxides as generally observed in the fingerprint region of 1000 cm^{-1}. The peaks observed at 617.98 cm^{-1} and 839.73 cm^{-1} confirmed the presence of ZnO.[33] The large bands observed at 3909 cm^{-1} and 3778.57 cm^{-1} were due to the O–H stretching of PVA. The peaks observed at 1639 cm^{-1}, 1572 cm^{-1} and 1256 cm^{-1} confirmed the presence of CAT enzyme.[34] The peaks observed at 2933.56 cm^{-1} and 1413.53 cm^{-1} correspond to C–H and C–C stretch of PVA respectively.[35] The peaks observed at 2380.32 cm^{-1} and 2149.43 cm^{-1} were due to the C–H stretch of chitosan and the adsorption peak at 3424.98 cm^{-1} was due to the N–H stretch of chitosan.[36] All the results obtained from the FT-IR spectrum of Au/ZnO-PVA/CAT/Chitosan confirmed the immobilization of CAT and chitosan on to the surface of ZnO-PVA nanocomposites.

3.3. Structural Characterization of ZnO-PVA Nanocomposites

X-ray diffraction pattern (XRD) of ZnO-PVA is shown in Figure 2(e). The characteristic diffraction peaks of PVA obtained at $2\theta = 14.107°$, 18.624°, 27.206°, 40.531° and 42.338° corresponding to (001), (101), (201), (110) and (211) planes confirmed the presence of PVA in ZnO-PVA nanocomposites. Diffraction peaks for ZnO were clearly observed at $2\theta = 33.304°$, 46.855°, 56.56°, 71.021° and 77.57°, which can be assigned to (002), (102), (110), (004) and (202) planes confirming the presence of ZnO with hexagonal wurtzite structure. The obtained planes of ZnO matched with the Joint Committee for Powder Diffraction Standards [JCPDS Card No. 36-1451].

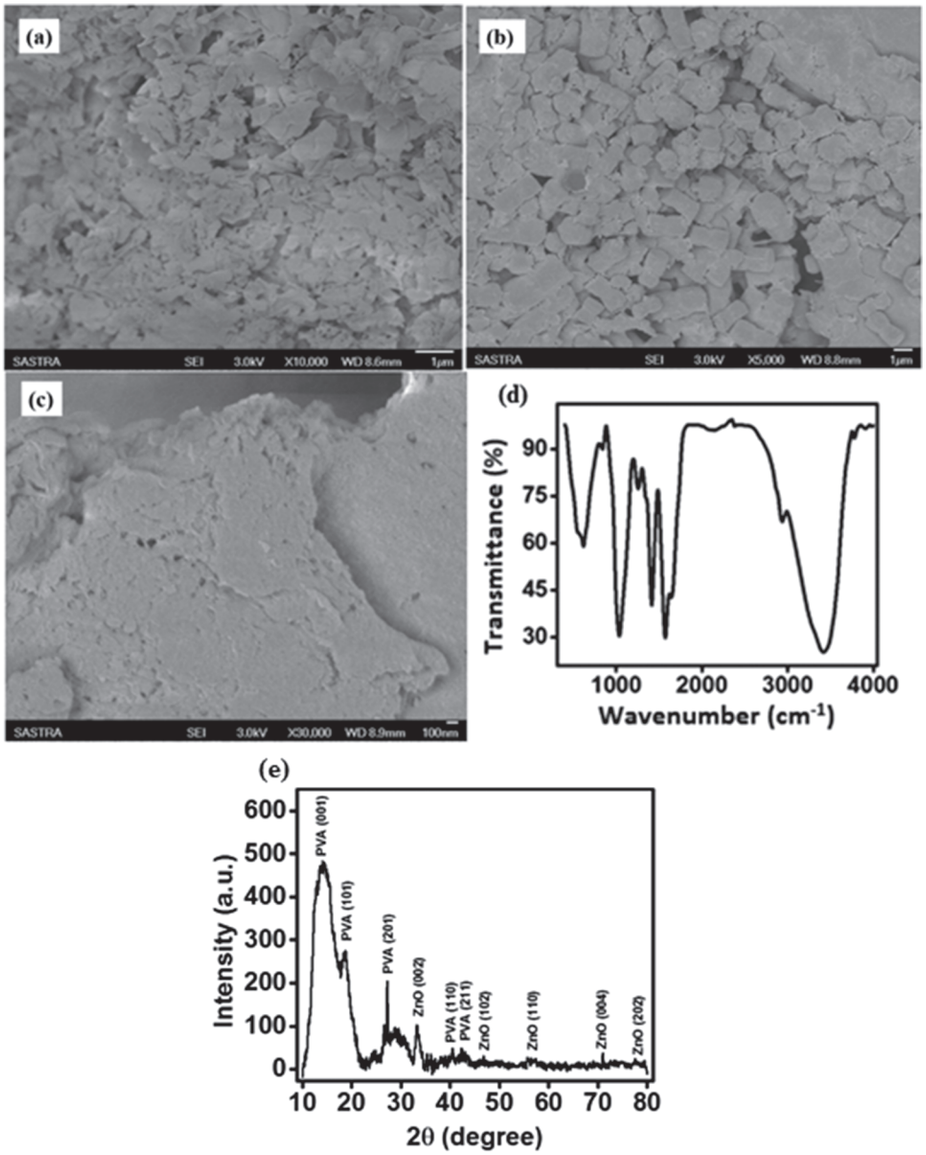

Figure 2. FE-SEM images of (a) ZnO-PVA, (b) ZnO-PVA/CAT and (c) ZnO-PVA/CAT/Chitosan, (d) FT-IR spectrum of ZnO-PVA/CAT/Chitosan and (e) XRD pattern of ZnO-PVA.

3.4. Optimization of Experimental Variables for H_2O_2 Detection

3.4.1. Electrochemical Reaction Mechanism at the Various Modified Au Electrode Surface

Cyclic voltammetric response of different electrodes namely (i) bare Au, (ii) Au/CAT/Chitosan and (iii) Au/ZnO-PVA/CAT/Chitosan were tested in PBS (pH 7.4, 0.1 M) containing 1 μM H_2O_2 performed at a scan rate of 1.01 Vs^{-1} is shown in Figure 3(a).

No redox peak current was noticed at bare Au electrode, suggesting that there was no catalytic activity in the applied potential range (Fig. 3(a)). When compared to the redox current densities of Au/CAT/Chitosan bio-electrode, the current density of Au/ZnO-PVA/CAT/Chitosan bio-electrode was increased by 6%. This might be due to the synergic effect of ZnO and PVA in the ZnO-PVA nanocomposites. The increase in redox peak current can be attributed to the high sensitivity of Au/ZnO-PVA/CAT/Chitosan bio-electrode towards H_2O_2. It also showed that the CAT enzyme was effectively immobilized on the surface of Au/ZnO-PVA working electrode.

The response of various modified electrodes towards electrochemical parameters were studied to investigate the electrochemical reaction mechanism that occurs on the surface of the Au/ZnO-PVA/CAT/Chitosan electrode. The interaction of H_2O_2 with the immobilized CAT on the

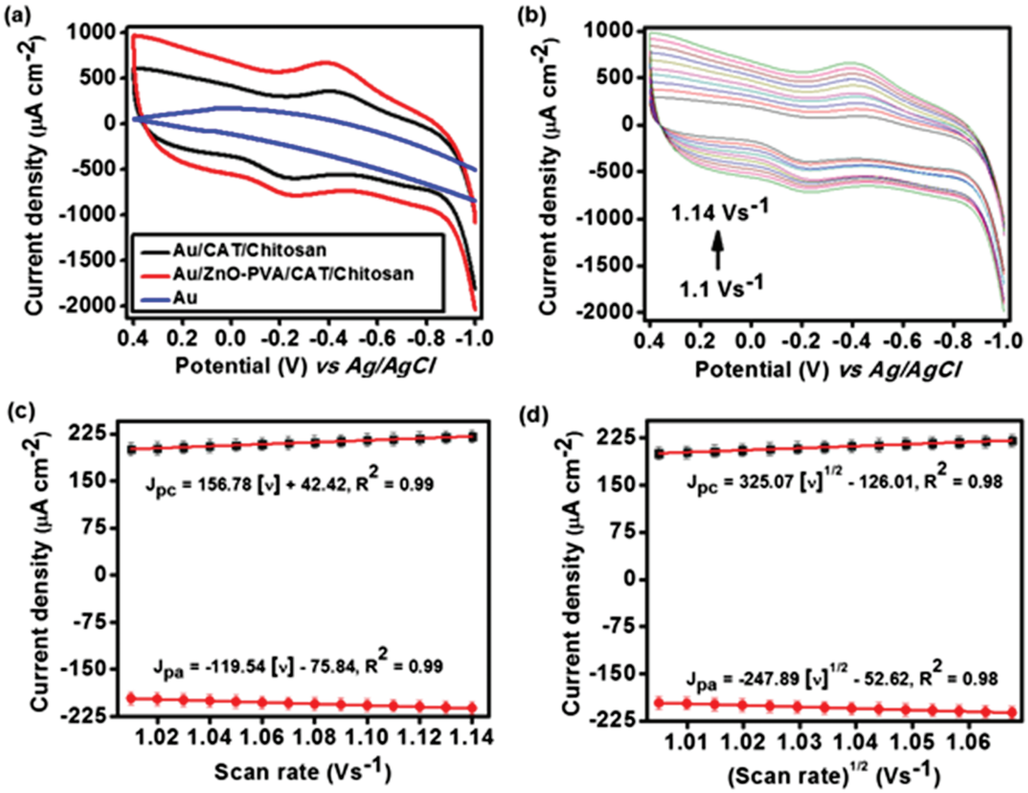

Figure 3. (a) Cyclic voltammetric response of various Au modified electrodes in PBS (pH 7.4, 0.1 M) containing 1 μM H_2O_2 performed at a scan rate of 1.01 Vs^{-1}, (b) cyclic voltammograms of Au/ZnO-PVA/CAT/Chitosan bio-electrode at different scan rates in the presence of 1 μM H_2O_2 in PBS (0.1 M, pH 7.4), (c) the plot of peak current density versus scan rate and (d) the plot of peak current density versus square root of scan rate.

surface of Au electrode was studied using cyclic voltammetry. Initially, the Au/CAT/Chitosan bio-electrode was analyzed in the potential between 0.4 V and −1.0 V. At approximately −0.259 V (vs. Ag/AgCl), Au/CAT/Chitosan electrode reduced Fe^{3+} to Fe^{2+}, present in the catalytic site of CAT enzyme, which was then subjected to anodic reduction at −0.408 V (Ag/AgCl). H_2O_2 got oxidized at −0.408 V to form O_2 and H_2O resulting in an effective electron transfer between the CAT enzyme and Au working electrode. Similar electrochemical reaction occurs in the Au/ZnO-PVA/CAT/Chitosan bio-electrode. The biochemical reactions of Au/CAT/Chitosan, Au/ZnO-PVA/CAT/Chitosan involved in the electrochemical measurements are listed as follows:

$$\mathrm{Fe(III)_{CAT}} + e^- \rightarrow \mathrm{Fe(II)_{CAT}}$$

$$\mathrm{H_2O_2} \rightarrow \frac{1}{2}\mathrm{O_2} + \mathrm{H_2O} + e^-$$

The cathodic and anodic potentials of Au/CAT/Chitosan, Au/ZnO-PVA/CAT/Chitosan were located at −0.259 and −0.408 V, −0.259 and −0.390 V with ΔE_p of 0.149 and 0.131 V respectively, which depicted the characteristic redox potential couple of Fe(III):Fe(II) and H_2O_2: 1/2 O_2 electroactive species respectively.

3.4.2. Change in Peak Potentials of Chemically Modified Au Bio-Electrodes

Comparing with Au/CAT/Chitosan (ΔE_p = 0.149 V), the change in peak potential (ΔE_p) of Au/ZnO-PVA/CAT/Chitosan was smaller with a value of 0.131 V (vs. Ag/AgCl), which is lesser than 0.200 V (vs. Ag/AgCl). The separation between the peak potential observed in the Au/ZnO-PVA/CAT/Chitosan was 0.018 V lesser than that of Au/CAT/Chitosan bio-electrode, which can be attributed to the perfect orientation of immobilized CAT biomolecules on ZnO-PVA nanocomposites. The separation between the cathodic and anodic peaks showed the quasi reversible nature and fast electron transfer process occurred at the surface of Au/ZnO-PVA/CAT/Chitosan bio-electrode.

3.4.3. Formal Potential of Various Modified Au Bio-Electrodes

The formal potential ($E^o = (E_{pc} + E_{pa})/2$, where E_{pa} and E_{pc} are the anodic and cathodic potential respectively) of Au/CAT/Chitosan bio-electrode was found to be −0.333 V (vs. Ag/AgCl), which was higher than that of Au/ZnO-PVA/CAT/Chitosan (−0.324 V vs. Ag/AgCl). The formal potentials of these modified Au electrodes were found to be lesser than that of formal potentials of multi-walled carbon nanotubes modified glassy carbon electrode

Table I. Electrochemical parameters estimated from the cyclic voltammograms of different modified Au electrodes in PBS (pH 7.4, 0.1 M) for 1 μM H_2O_2.

	I_p (μA cm^{-2})		E_p (V)			K_s (s^{-1})		Γ ($\times 10^{-9}$ M cm^{-2})	
Electrode	Cathode	Anode	Cathode	Anode	ΔE_p (V)	Cathode	Anode	Cathode	Anode
Au	–	–	–	–	–	–	–	–	–
Au/CAT/Chitosan	193.59	185.26	−0.408	−0.259	0.149	3.87	3.74	7.20	7.86
Au/ZnO-PVA/CAT/Chitosan	200.57	196.32	−0.390	−0.259	0.131	4.89	4.86	8.25	9.54

(MWCNTs-NF-CAT, $E^o = -0.380$ V vs. Ag/AgCl).[37] This showed that the ZnO-PVA nanocomposites improved the contact between the CAT enzyme and Au working electrode and decreased the working potential for the redox reaction by retaining the catalytic activity of CAT enzyme.

3.4.4. Electron Transfer Rate Constant

Electrochemical parameters estimated from the cyclic voltammetry of different modified Au electrodes in PBS (pH 7.4, 0.1 M) for 1 μM H_2O_2 is given in Table I. The electron transfer rate constants ($K_s = I_p/Q$, where K_s is the electron transfer rate constant and Q is the amount of charge consumed) of CAT enzyme immobilized on Au/ZnO-PVA/CAT/Chitosan bio-electrode in the cathodic and anodic processes were calculated as 4.89 s^{-1} and 4.86 s^{-1}, which were found to be higher than the value reported for the CAT enzyme immobilized on Au/CAT/Chitosan electrode (K_s in cathode = 3.87 s^{-1}; K_s in anode = 3.74 s^{-1}) demonstrated the enhanced electron transfer rate by ZnO-PVA nanocomposites during the electrochemical process.

3.4.5. Surface Coverage of Adsorbed Electroactive H_2O_2

The surface coverage of adsorbed electroactive H_2O_2 biomolecule on Au/CAT/Chitosan and Au/ZnO-PVA/CAT/Chitosan was calculated using the formula, $\Gamma = I_p(\text{irrev.})2.718\text{RT}/(n\alpha n_a F^2 A\nu)$, where surface coverage (Γ) denotes the surface density of adsorbed H_2O_2, T denotes the room temperature, I_p (irrev.) is the irreversible peak current, n_a is the number of electrons involved in the charge transfer step, F is the Faraday's constant, R is the gas constant, ν is the scan rate, n is the number of electrons in the redox reaction, A is the area of Au working electrode and α is the electron transfer coefficient. The concentration of electroactive H_2O_2 bio-molecule adsorbed on to the surface of Au/CAT/Chitosan bio-electrode and Au/ZnO-PVA/CAT/Chitosan were found to be 7.20×10^{-9} M cm^{-2} and 7.86×10^{-9} M cm^{-2}. Compared to Au/CAT/Chitosan, Au/ZnO-PVA/CAT/Chitosan exhibited a higher surface coverage due to the large surface area of ZnO-PVA nanocomposite. Hence, an increase in current value was achieved using Au/ZnO-PVA/CAT/Chitosan. Comparing to Au/CAT/Chitosan bio-electrode, the surface coverage of adsorbed H_2O_2 bio-molecules on Au/CAT/Chitosan bio-electrode and Au/ZnO-PVA/CAT/Chitosan was higher in the cathodic (8.25×10^{-9} M cm^{-2}) and the anodic (9.54×10^{-9} M cm^{-2}) processes respectively. The increase in surface coverage of H_2O_2 might be due to the large surface area of ZnO-PVA nanocomposites.

3.4.6. Influence of Scan Rate on the Electrochemical Behaviour of Au/ZnO-PVA/CAT/Chitosan Bio-Electrode

The effect of scan rate on the electrochemical behaviour of Au/ZnO-PVA/CAT/Chitosan bio-electrode is shown in Figure 3(b). The applied scan rate ranges from 1.01 Vs^{-1} to 1.14 Vs^{-1}. From the results of adjusted regression coefficient (R^2), it was clear that the cathodic and anodic peak current densities were dependent on the applied scan rate ($R^2 = 0.99$) (Fig. 3(c)) and not on the applied square root of scan rate ($R^2 = 0.98$) (Fig. 3(d)). The cathodic (J_{pc} (μA cm^{-2}) = 156.78 [ν] (μA cm^{-2}/Vs^{-1}) + 42.42, $R^2 = 0.99$) and the anodic peak current density (J_{pa} (μA cm^{-2}) = −119.54 [ν] (μA cm^{-2}/Vs^{-1}) − 75.84, $R^2 = 0.99$) increased linearly with the scan rate ranging from 1.01 Vs^{-1} to 1.14 Vs^{-1} (Fig. 3(c)) and it was obvious that electroactive H_2O_2 adsorbed onto the Au/ZnO-PVA/CAT/Chitosan bio-electrode undergone a surface controlled electron transfer process rather than a diffusion controlled process.

3.5. Effect of Increasing H_2O_2 Concentration

Cyclic voltammetry curves of Au/ZnO-PVA/CAT/Chitosan bio-electrode for increasing H_2O_2 concentration in 0.1 M PBS (pH = 7.4) at 1.01 Vs^{-1} are shown in Figure 4(a). The current density found in the cathodic (J_{pc} (μA cm^{-2}) = 219.45 [H_2O_2] (μM) + 1.81, $R^2 = 0.99$) and the anodic processes (J_{pa} (μA cm^{-2}) = −210.06 [H_2O_2] (μM) − 1.47, $R^2 = 0.99$) showed good linearity between 1 μM and 17 μM (Fig. 4(b)). The LOD was found to be 9.13 nM and it was estimated using the formula, LOD = $(3.3 \times S)/S$, where S is the standard deviation in the absence of H_2O_2 (0.582 μA cm^{-2}) and S is the slope of calibrated curve in presence of H_2O_2 (210.06 μA cm^{-2} μM^{-1}). In addition, limit of quantification (LOQ = $(10 \times S)/S$) was calculated to determine lowest concentration of H_2O_2 in human blood serum with suitable precision and accuracy. The LOQ was estimated as 30 nM.

The maximum current density ($J_{\max}$) and Michaelis-Menten constant (K_M) were calculated as 0.39 μM

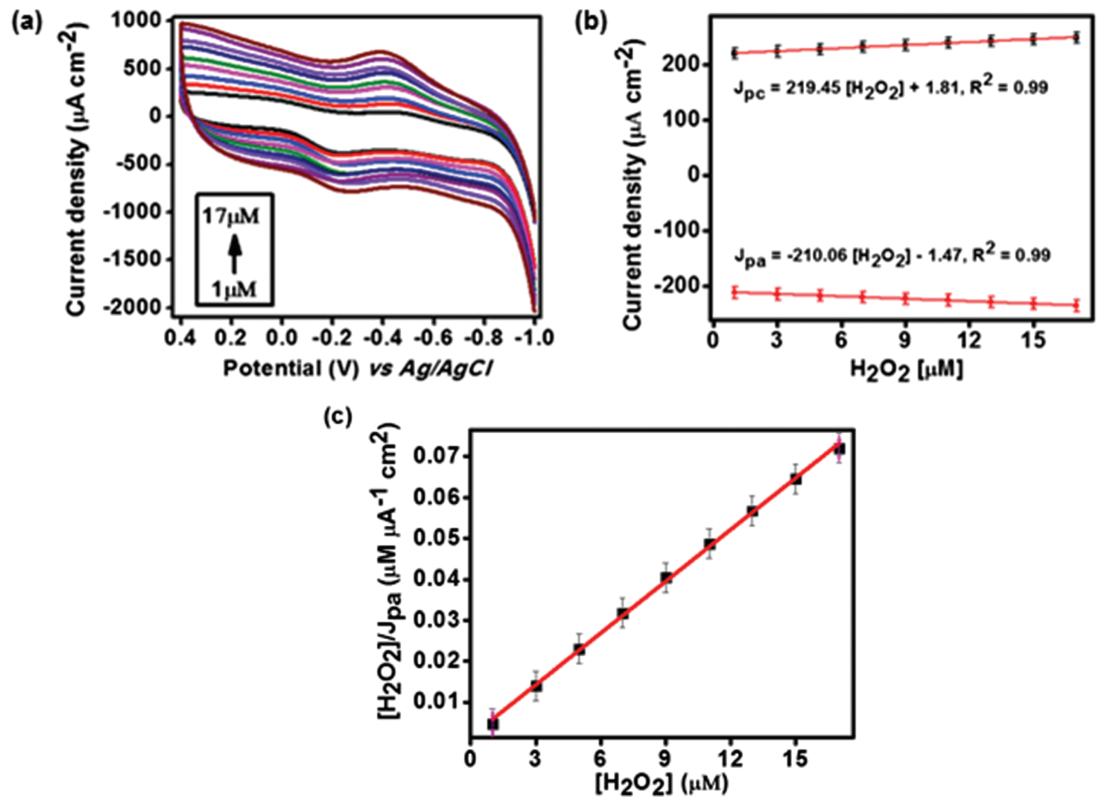

Figure 4. (a) Cyclic voltammetric curves of Au/ZnO-PVA/CAT/Chitosan bio-electrode for increasing H_2O_2 in PBS at 1.14 Vs^{-1} (0.1 M, pH 7.4), (b) calibration curves of Au/ZnO-PVA/CAT/Chitosan bio-electrode for the varying concentration of H_2O_2 in PBS (0.1 M, pH 7.4) and (c) H_2O_2 concentration/current density response versus H_2O_2 concentration plot (Hanes-Woolf plot).

and 237.53 μA cm^{-2} respectively (Fig. 4(c)). The estimated K_M value was found to be lower than that of immobilized CAT enzyme on Fe_3O_4-MWCNT/Au electrode (0.6 μM),[22] MWCNT/GC electrode (1.7 mM),[38] CACNT/GC electrode (0.21 mM).[39] This low K_M revealed the good affinity between the immobilized CAT enzyme and added H_2O_2 biomolecules.

3.6. Response Time

Response time is the time needed for Au/ZnO-PVA/CAT/Chitosan bioelectrode to reach 95% of its stable value. In order to evaluate the response time, amperometry was performed in 1 μM H_2O_2 at an applied potential of -0.259 V (vs. Ag/AgCl). The response time of the developed H_2O_2 biosensor was calculated to be less than 1 s. The fast response time of the proposed biosensor was due to the enhanced electron transfer property of ZnO-PVA nanocomposites. When the response time of the developed H_2O_2 biosensor was compared (Table II) with other reported H_2O_2 biosensors, it was apparent that the Au/ZnO-PVA/CAT/Chitosan bioelectrode possessed a lower response time of less than 1 s.

3.7. Repeatability and Reproducibility

Repeatability and reproducibility for intra- and inter-assay were determined from analysis of variance (ANOVA) and relative standard deviation (RSD) at 1 μM of H_2O_2 in 0.1 M of PBS (pH 7.4) using Au/ZnO-PVA/CAT/Chitosan ($n = 10$) bio-electrode. The RSD of inter- and intra-assay was found to be 1.82% and 0.91% respectively. At 0.05 level ($P > 0.05$), the mean current density for Au/ZnO-PVA/CAT/Chitosan was not significantly different, suggesting good embedding between CAT enzyme and ZnO-PVA nanocomposites. In order to see any significant mean difference between the reproduced current density ($n = 10$), Two-way ANOVA was performed.

Table II. Comparison of response time of Au/ZnO-PVA/CAT/Chitosan electrode with the previously reported response time values of CAT based H_2O_2 biosensors.

Working electrode	Sensor type	Nano-interface	Linear range (μM)	Response time (s)	References
CAT/MWCNT/ Nafion/GCE	Cyclic voltammetry	MWCNT	10–5000	2	[40]
CAT/ChOx/ GR-IL/GCE	Cyclic voltammetry	Gelatin	0.25–215	6	[41]
CAT/CACNT	Cyclic voltammetry	CACNT	10–3200	4	[39]
Au/ZnO-PVA/ CAT/Chitosan	Cyclic voltammetry	ZnO-PVA	1–17	<1	Present work

The mean difference between the reproduced current density was not significantly different at 0.05 level ($P > 0.05$). The obtained results confirmed the standard fabrication of Au/ZnO-PVA/CAT/Chitosan electrode.[42]

3.8. Interferents Study

Interferent studies were performed to check the specificity of the developed biosensor. The interferent of ascorbic acid (0.01 mM), lactic acid (0.01 mM), urea (0.01 mM) and glucose (0.01 mM) towards the CAT enzyme response was studied in the presence of 1 μM of H_2O_2. The percentage inhibition was estimated using the following Eq. (1).

$$I\% = \frac{J_o - J_i}{J_o} \times 100 \tag{1}$$

where, J_o and J_i are the obtained current densities in the absence and presence of inhibitor respectively. The addition of ascorbic acid, lactic acid, urea and glucose didn't alter the current density response over the Au/ZnO-PVA/CAT/Chitosan bio-electrode's detection limit. These results also manifested that the chitosan modified Au/ZnO-PVA/CAT bio-electrode can effectively avoid the interferent of the ascorbic acid ($I\% = 0.72\%$), lactic acid ($I\% = 1.05\%$), urea ($I\% = 1.52\%$) and glucose ($I\% = 1.21\%$).

3.9. Stability

The stability of Au/ZnO-PVA/CAT/Chitosan was calculated using Eq. (2),

$$\%\text{Stability} = \frac{J_n - J_o}{J_o} \times 100 \tag{2}$$

where, J_n and J_o are the obtained current densities in the 'n'th day and first day respectively. The dry stability of the developed H_2O_2 biosensor was checked for 20 days at room temperature. The Au/ZnO-PVA/CAT/Chitosan bio-electrode retained 93% of its original current density over a storage period of 20 days, which was attributed to the strong interaction between ZnO-PVA nanocomposites and CAT enzyme.

3.10. Application

The practicability of the fabricated Au/ZnO-PVA/CAT/Chitosan bio-electrode was tested in the human blood serum sample (Table III). To test the recovery and RSD, 5 mL of human blood sample was collected and the serum was separated by centrifugation at 2500 rpm for 5 min. 20 μL human blood serum stock solution was diluted in PBS (0.1 M, pH 7.4) and the known concentrations of H_2O_2 (0.2 μM, 0.4 μM, 0.6 μM, 0.8 μM, 1 μM) was added in triplicates. Recovery % of H_2O_2 from human blood serum sample ranged between 95% and 106.66% with RSD of <4.56%. This depicted that the developed Au/ZnO-PVA/CAT/Chitosan bio-electrode had the ability to overcome the potential interferents present in the human blood serum samples. And, the low RSD of <4.56% indicated that the repeatability and reproducibility of the developed H_2O_2 biosensor were good.

Table III. Determination of H_2O_2 in human blood serum samples.

H_2O_2 added (μM)	H_2O_2 predicted (μM)	Recovery (%)	Relative standard deviation (%RSD)
0	1.6	–	–
0.2	1.79	95	3.63
0.4	2.18	97.5	1.79
0.6	2.82	106.6	4.56
0.8	3.61	98.7	0.89
1	4.58	97	2.15

4. CONCLUSION

In this work, a cyclic voltammetric method was developed for the detection of H_2O_2 in human blood serum sample using the fabricated Au/ZnO-PVA/CAT/Chitosan bio-electrode. The cyclic voltammetric response of Au/ZnO-PVA/CAT/Chitosan showed enhanced surface coverage and fast electron transfer between the immobilized CAT enzyme and Au working electrode. The developed biosensor exhibited high sensitivity (210 μA cm^{-2}), rapid response time (<1 s) and low LOD (9.13 nM). Moreover, the immobilized CAT enzyme on the ZnO-PVA nanocomposite modified Au electrode showed acceptable recovery towards H_2O_2 determination. All these results demonstrated that the fabricated Au/ZnO-PVA/CAT/Chitosan bio-electrode can be used as a sensing element in hand-held portable system for the detection of H_2O_2 in human blood serum sample.

Acknowledgment: The authors are grateful to the Department of Science and Technology, New Delhi, for their financial support (DST/TSG/PT/2008/28, SR/FST/ETI-284/2011(C) SR/FST/LSI-453/2010 and DST/TM/WTI/2K14/197(a)(G) and (Nano Mission Council (No. SR/NM/PG-16/2007)). We also acknowledge SASTRA University, Thanjavur for extending infrastructural support to carry out the study.

References and Notes

1. E. A. Veal, A. M. Day, and B. A. Morgan, *Mol. Cell.* 26, 1 (**2007**).
2. M. Kim, H. Chung, and M. S. Kemper, *J. Pharm. Biomed. Anal.* 48, 592 (**2008**).
3. T. Moreno, M. A. M. Lopez, I. H. Illera, C. M. Piqueras, A. S. Arranz, J. G. Serna, and M. J. Cocero, *Chem. Eng. J.* 166, 1061 (**2011**).
4. N. St Hill and G. Turner, *Anal. Methods.* 3, 1901 (**2011**).
5. L. C. Chen, Z. Yu, and K. Hiraoka, *Anal. Methods.* 2, 897 (**2010**).
6. C. A. Marquette, B. D. Leca, and L. J. Blum, *Luminescence* 16, 159 (**2001**).
7. M. Xu, B. R. Bunes, and L. Zang, *ACS Appl. Mater. Interfaces.* 3, 642 (**2011**).
8. M. Schaferling, D. B. M. Grogel, and S. Schreml, *Microchim. Acta* 174, 1 (**2011**).

9. H. J. Jiang, H. Yang, and D. L. Akins, *J. Electroanal. Chem.* 623, 181(**2008**).
10. M. Baccarin, B. C. Janegitz, R. Berte, F. C. Vicentini, C. E. Banks, O. Fatibello-Filho, and V. Zucolotto, *Mater. Sci. Eng. C* 58, 97 (**2016**).
11. L. Wang, J. Wang, and F. Zhou, *Electroanal.* 16, 627 (**2004**).
12. L. Xie, Y. Xu, and X. Cao, *Colloids Surf. B* 107, 245 (**2013**).
13. A. B. M. Zakaria, and D. Leszczynska, *J. Electroanal. Chem.* 766, 30 (**2016**).
14. P. Kanyong, S. Rawlinson, and J. Davis, *J. Electroanal. Chem.* 766, 147 (**2016**).
15. X. Zhang, D. Liu, B. Yu, and T. You, *Sensors Actuators, B Chem.* 224, 103 (**2016**).
16. L. Mei, P. Zhang, J. Chen, D. Chen, Y. Quan, N. Gu, G. Zhang, and R. Cui, *Microchim. Acta* 183, 1359 (**2016**).
17. H. Mei, W. Wu, B. Yu, H. Wu, S. Wang, and Q. Xia, *Sensors Actuators, B Chem.* 223, 68 (**2016**).
18. D. Chirizzi, M. R. Guascito, E. Filippo, C. Malitesta, and A. Tepore, *Talanta.* 147, 124 (**2016**).
19. K. Barman and S. Jasimuddin, *RSC Adv.* 6, 20800 (**2016**).
20. J. Zhou, C. Liao, L. Zhang, Q. Wang, and Y. Tian, *Anal. Chem.* 86, 4395 (**2014**).
21. S. Wang, F. Xie, and G. Liu, *Talanta* 77, 1343 (**2009**).
22. K. Thandavan, S. Gandhi, N. Nesakumar, S. Sethuraman, J. B. B. Rayappan, and U. M. Krishnan, *Sensors Actuators, B Chem.* 215, 166 (**2015**).
23. S. F. Wang, T. Chen, Z. L. Zhang, D. W. Pang, and K. Y. Wong, *Electrochem. Commun.* 9, 1709 (**2007**).
24. Y. Yang, G. Yang, Y. Huang, H. Bai, and X. Lu, *Colloids Surfaces A Physicochem. Eng. Asp.* 340, 50 (**2009**).
25. A. Mehta, S. Patil, H. Bang, H. J. Cho, and S. Seal, *Sensors Actuators A Phys.* 134, 146 (**2007**).
26. S. Chen, R. Yuan, Y. Chai, L. Zhang, N. Wang, and X. Li, *Biosens. Bioelectron.* 22, 1268 (**2007**).
27. K. Thandavan, S. Gandhi, S. Sethuraman, J. B. B. Rayappan, and U. M. Krishnan, *Nanotechnol.* 22, 1 (**2011**).
28. Z. Yang, X. Zong, Z. Ye, B. Zhao, Q. Wang, and P. Wang, *Biomater.* 31, 7534 (**2010**).
29. Y. Zhang, Y. Zhang, H. Wang, B. Yan, G. Shen, and R. Yu, *J. Electroanal. Chem.* 627, 9 (**2009**).
30. S. W. Tan, X. C. Tan, J. Y. Jiang, J. Xu, J. L. Zhang, D. D. Zhao, L. Liu, and Z. Y. Huang, *J. Electroanal. Chem.* 668, 113 (**2012**).
31. Q. Li, K. Cheng, W. Weng, P. Du, and G. Han, *Thin Solid Films* 544, 466 (**2013**).
32. R. Rahmanian and S. A. Mozaffari, *Sens. Actuators, B Chem.* 207, 772 (**2015**).
33. H. Kumar and R. Rani, *Int. Lett. Chem. Phys. Astron.* 14, 26 (**2013**).
34. N. Ellina, N. Izaanin, J. Abdullah, N. Arif, and N. Azah, *Biosens. Bioelectron.* 61, 1 (**2014**).
35. K. S. Hemalatha, K. Rukmani, N. Suriyamurthy, and B. M. Nagabhushana, *Mater. Res. Bull.* 51, 438 (**2014**).
36. N. Nesakumar, S. Sethuraman, U. M. Krishnan, and J. B. B. Rayappan, *J. Appl. Electrochem.* 46, 309 (**2016**).
37. P. A. Prakash, U. Yogeswaran, and S. M. Chen, *Talanta* 78, 1414 (**2009**).
38. A. Salimi, A. Noorbakhsh, and M. Ghadermarz, *Anal. Biochem.* 344, 16 (**2005**).
39. A. P. Periasamy, Y. Ho, and S. Chen, *Biosens. Bioelectron.* 29, 151(**2011**).
40. P. Vatsyayan, S. Bordoloi, and P. Goswami, *Biophys. Chem.* 153, 36 (**2010**).
41. M. Bagher and M. Khodadadian, *Biosen Bioelectron.* 53, 472 (**2014**).
42. Y. Lin and H. S. Nalwa (eds.), Handbook of Electrochemical Nanotechnology, American Scientific Publishers, Los Angeles, CA (**2009**), Vols. 1–2.

Received: 17 August 2016. Accepted: 17 July 2017.